Road Terrain Type Classification based on Laser Measurement System Data

Shifeng Wang
Centre for Autonomous Systems (CAS),
Faculty of Engineering and IT, University of Technology Sydney (UTS),
15 Broadway, NSW, 2007, Australia.
Shifeng.Wang@student.uts.edu.au
Sarath Kodagoda
Centre for Autonomous Systems (CAS),
Faculty of Engineering and IT, University of Technology Sydney (UTS),
15 Broadway, NSW, 2007, Australia.
Sarath.Kodagoda@uts.edu.au
Ravindra Ranasinghe
Centre for Autonomous Systems (CAS),
Faculty of Engineering and IT, University of Technology Sydney (UTS),
15 Broadway, NSW, 2007, Australia.
Ravindra.Ranasinghe@uts.edu.au

Abstract

For road vehicles, knowledge of terrain types is useful in improving passenger safety and comfort. The conventional methods are susceptible to vehicle speed variations and in this paper we present a method of using Laser Measurement System (LMS) data for speed independent road type classification. Experiments were carried out with an instrumented road vehicle (CRUISE), by manually driving on a variety of road terrain types namely Asphalt, Concrete, Grass, and Gravel roads at different speeds. A looking down LMS is used for capturing the terrain data. The range data is capable of capturing the structural differences while the remission values are used to observe anomalies in surface reflectance properties. Both measurements are combined and used in a Support Vector Machines Classifier to achieve an average accuracy of 95% on different road types.

1 Introduction

Road terrain type classification based on on-board sensors can provide important, sometimes crucial information regarding safety, fuel efficiency and passenger comfort. It can be used to estimate various physical quantities including friction coefficients, slip angles and vehicle handling characteristics [Iagnemma, 2004] [Nohse, 1991] [Shmulevich, 1996]. Therefore estimation of road surface parameters is of interest in many mobile vehicle applications.

Road terrain type classification methods have been extensively studied in the past. Algorithms based on various sensory modules, such as Laser Measurement Systems, cameras, accelerometers, GPS, and wheel encoders have been reported. Being one of the most reliable sensors, LMS is used in autonomous robots for avoiding dangerous paths [Stavens, 2006] [Dahlkamp, 2006] altogether.

Apart from range information provided by LMS, remission information of the laser beam is also available in some types of laser models. The method in [Wurm, 2009] has been reported to use laser remission values to identify vegetation on structured environments. The approach in [Saitoh, 2010] proposed a method to define a hazard and un-drivable area by using self-supervised learning based on the remission value of a map. However, these two methods find drivable regions but not the road terrain types.

Varieties of road terrain types have abundant different characteristics. Vehicle vibrations while driving on such surfaces could be thought as the most naïve data to be used for identifying different road terrain types [Brooks, 2005] [Komma, 2009]. Weiss et al [Weiss, 2007] used a vertically mounted accelerometer on the platform, RWI ATRV-Jr to classify some indoor and outdoor terrain types. Then the study extended to use an accelerometer and a camera for improved terrain type classification [Weiss, 2008]. Hsiao et al [Hsiao, 2009] and Helmick et al [Helmick, 2009] used images from cameras pointing down for road terrain type classification. The images were analysed to identify potholes and ruts to distinguish different road terrain types. However, both of the research works were based on small sized robotic platform operating at slow speeds. The stability of this method was affected by lack of camera's exposure time to capture fast moving features or low illuminated backgrounds [Wang, 2011].

The approaches mentioned above are

implemented on small sized robotic platforms that have rigid wheels providing a good coupling between the terrain and the rover. Those methods cannot be readily used in road vehicles due to various dampers including the tyres and shock-absorbers. Therefore, in [Ward 2009], they utilized the dynamic model of the vehicle with a vertically mounted accelerometer to reconstruct the road surface. As the road surface is independent of the vehicle speed, frequency domain features were extracted for terrain type classification. However, further research [Wang, 2012] showed that it has limitations due to non-ideal nature and parametric uncertainties of the model resulting in speed dependency.

This paper focuses on road terrain type classification using LMS, which provides range and remission values at a high sampling rate. Thereby, spatial frequency features of the lateral direction can be extracted for road terrain classification.

The paper is arranged as follows. Section 2 describes the road surface estimation procedure and the feature extraction methodology. Section 3 presents the details of the classifier and in Section 4 experimental platform is described followed by experimental results. Section 5 concludes the paper indicating future direction of the research.

2 Methodology

2.1 Geometric Arrangement of the LMS

A downward-looking SICK LMS111 is mounted on the CRUISE as shown in Fig. 1. It scans the road surface vertically in a two dimensional plane at a 50 Hz sampling rate. The LMS has a 270° field of view with 0.5° angular resolution providing 541 range and remission values per scan. While the vehicle is moving forward, it leaves a trace of three dimensional point cloud of the surface.

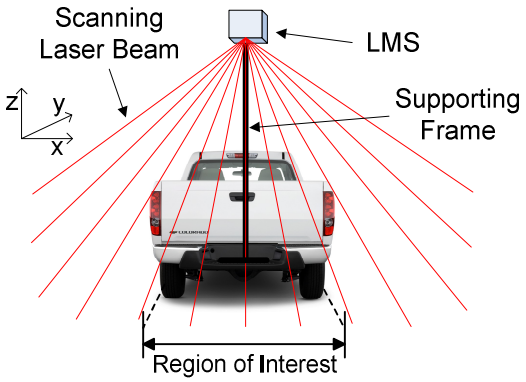

Fig. 1 The geometric arrangement of the LMS

2.2 Reconstruction of the Road Surface

It is well known that the laser beam emitted in a LMS is deflected using a rotating mirror and scans surroundings in a circular manner. In general, once a laser beam incidents on a surface, the light is reflected. This reflected energy can be partly received by the photodiode in the LMS calculating the range to an object based on time of flight measurements.

As shown in Fig. 2, the surface is estimated by the laser range data and the speed data coming from the GPS unit.

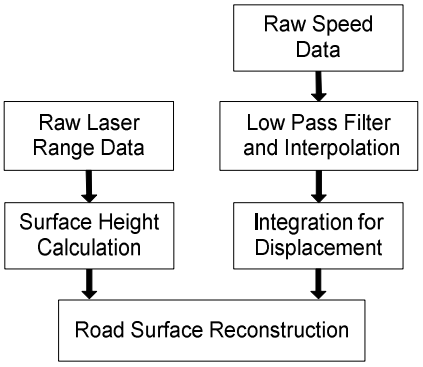

Fig. 2 Reconstruction of the Road Surface

Range Data Processing

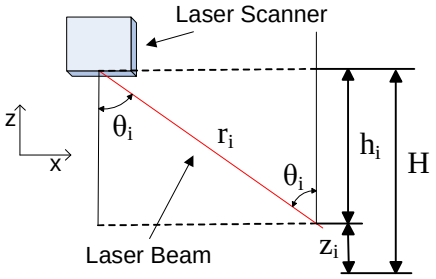

Fig. 3 Mounting geometry of the LMS

Vertical coordinate, z_i, of each range measurement can be easily reconstructed by (See Fig. 3):

$$z_i = H - r_i \cos(\theta_i) \tag{1}$$

where, r_i is laser range value, θ_i is included angle between the current laser beam and z axis, and H is the reference height from a relatively flat floor to the height of the LMS. In a similar way, the x-axis coordinate can be calculated as:

$$x_i = r_i \sin(\theta_i) \tag{2}$$

The 270° scanning field of view contains road surface as well as other nearby objects. Therefore, as illustrated in Fig. 1, a 1.3m wide region of interest is defined for the purpose. This leads to inter-distance between two sampling points of a particular scan to approximately be 2 centimetres on a road surface with the mounted height 2.2 meters of the LMS.

Speed Data Processing

The 20Hz Global Positioning System (GPS) on board is used to measure the speed of the vehicle. Although the experiments were restricted in open outdoor areas, the GPS did not keep a clear and stable logging all the way for some unknown reasons. At some places, the logged speed data contained unreasonable errors, so a low pass filter was employed to remove them.

As the speed data rate was too slow when comparing with that of the LMS data, it was interpolated to 50 Hz by proximal interpolation method (also known as nearest-neighbour interpolation) [Watson, 1984]. Then, simply the longitudinal vehicle displacement, *y(t)*, is

estimated by,

$$y(t) = \int_0^t |v(t)|\, dt \qquad (3)$$

where *v(t)* is the estimated vehicle speed.

Road Surface

Once the data is processed to estimate the longitudinal and lateral displacements of the laser data point clouds, a three dimensional view of the displacements can be generated. Such displacement profiles of the road types are shown in Fig. 4. It seems not difficult to reconstruct a qualitative assessment of the plots for the differences purely by visual inspections.

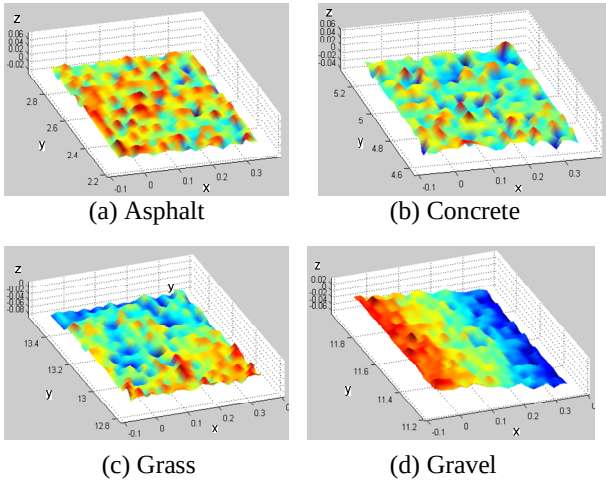

(a) Asphalt (b) Concrete

(c) Grass (d) Gravel

Fig. 4 Three dimensional surface data of four different road types.

2.3 Feature Matrix

Extraction of Spatial Frequency Features

The estimated 3D surface has more dissimilarity in the resolution along the vehicle moving direction due to the variations of the speed. However, the vehicle speed has minimal effect on the lateral data. Therefore, in this work, only the lateral components are considered. Rather than relying on each new lateral scan of data, this will concatenate a group of scans captured over the vehicle length, which is 4 metres. This is done for future comparisons with other sensor modalities. The number of scans depends on the vehicle's speed, however, in general, it is around 35~145 scans at speeds of 20~80 km/h.

The feature matrix is formed by carrying out the Fast Fourier Transform on each scan. The power spectral density (PSD) is then calculated using Welch's method [Welch, 1967]. The start frequency, end frequency and frequency step are empirically decided as 0 cycles/meter (c/m) to 35 c/m with 0.1 c/m interval, which led to optimal classification rate in many prior tests.

$$F = \begin{bmatrix} F_{s_1,f_1} & \cdots & F_{s_n,f_1} \\ \vdots & \ddots & \vdots \\ F_{s_1,f_m} & \cdots & F_{s_n,f_m} \end{bmatrix} \qquad (3)$$

Then the PSD of each group of scan, which defines the feature vector, is arranged column by column to form the feature matrix *F*, given in (3). In this matrix, every column refers to a feature vector (a group of scanning lines) while every row represents the features (PSD) extracted using the above procedure. For instance, in this case, F_{s_1,f_1} presents the PSD from 0 c/m to 0.1 c/m of the 1st group lines, while F_{s_n,f_1} presents the PSD from 0 c/m to 0.1 c/m of the nth group, and F_{s_n,f_m} presents the PSD from 34.5 c/m to the end 35 c/m of the n^{th} segment. Overall, the matrix, *F* contains *n* samples while each sample has *m* features. Each value of element in matrix (3) indicates a power at a particular investigated frequency forming the final feature matrix. After all it is normalized to reflect each row of *F* mapped to [0, 1].

Remission based Features

As introduced in [Wurm, 2009] and [Saitoh, 2010], a laser remission value is a function of distance, incidence angle and material. For our application, since the LMS is mounted on a frame above the vehicle and the fact that we are only interested in a small field of view, the factors of distance and incidence angle can be considered relatively constant. Therefore, the remission value seems informative for road surface classification.

Similar to the previous section, we segment scanning lines into groups with the same length, however rather than the range values means of the remission values are used. So the feature matrix is,

$$R = \begin{bmatrix} R_{s_1,r_1} & \cdots & R_{s_n,r_1} \\ \vdots & \ddots & \vdots \\ R_{s_1,r_m} & \cdots & R_{s_n,r_m} \end{bmatrix} \qquad (4)$$

As given in the matrix (4), each column refers to mean values of a group (a sample) of lines while each row represents the mean value of a specific angle. For instance, R_{s_1,r_1} presents the mean remission value of all first points of the lines belong to 1st group, while R_{s_n,r_1} presents the mean remission value of all last points of the lines belong to 1st group, and R_{s_n,r_m} presents the mean remission value of all last points of the lines belong to n^{th} segment. The matrix is finally normalized to reflect each row of *R* mapped to [0, 1].

2.4 Classification

A number of classifiers were evaluated. Comparing with Neural Network classifier and Naïve Bayes classifier, Support Vector Machines (SVM) presents the best classification accuracy for road terrain type classification task by several number of off-line tests. SVM conceptually finds a hyper plane which separates the d-dimensional data in to its best separable classes. However, in some cases, the training data is often not linearly separable. SVM introduces the notion of a "kernel induced feature space", which casts the data into a higher dimensional space where the data is separable. We used a

freely available, highly accepted machine learning tool kit, WEKA [Bouckaert, 2010] in the implementation.

3 Experimental Results

3.1 Platform

Fig. 5 CRUISE: the experimental vehicle

The experimental test bed, CRUISE: CAS Research Ute for Intelligence, Safety and Exploration (Fig. 5), developed in-house was used for experimentation. CRUISE is equipped with range of sensors including GPS, cameras, LMS, accelerometers and an IMU. Number of computers mounted in the back tray, connected via Ethernet, are used for data collection and logging. A separate battery bank provides the required power.

As shown on right side of Fig. 5, a SICK LMS111 is mounted on the vehicle looking down for scanning the road surface. It is aligned with the central axis of the vehicle and scanning plane is perpendicular to the ground.

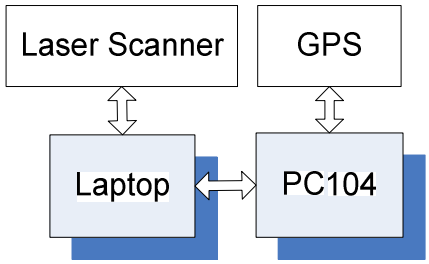

Fig. 6 The Hardware Structure of System

A laptop computer is used for laser data logging where as a PC104 computer logs the GPS data. Both computers are synchronized via Ethernet using NTP.

3.2 Data Collection

The experiment was performed in a fine day with average autumn temperature and humidity in an urban area of Sydney, Australia. CRUISE was driven on four types of roads, which were asphalt, concrete, grass, and gravel at different speeds while capturing data. Considering driving safety and practical constraints, the data was logged when the vehicle was driven on asphalt roads at speeds of 0-70 km/h, concrete roads at speeds of 30-40 km/h, grass roads at speeds of 10-20 km/h and gravel roads at speeds of 10-30 km/h, respectively. Critical vibration was felt by the passengers in the cab while running on grass roads over 20 km/h speeds, which was apparently not comfortable or safe for human and the vehicle with equipments. Data was collected along more than 30 km road segments. At least two people were required for the purpose, one was attending to data logging while the other was driving.

3.3 Experimental Results

The Speed Independency

The laser data collected were assumed to be minimally affected by the operating speed of the vehicle. This is reasonable as the LMS has a fast sampler which can capture range data in several microseconds.

This hypothesis was tested with data captured on Asphalt and Gravel roads at a range of different speeds. While the classifier was trained at a particular speed, it was tested at a different speed on the same road type. As shown in Table 1, the data set was divided into training and testing parts. It could be noted that the asphalt roads were the most widely available road type whereas concrete and grass roads were rare to find in Sydney.

Table 1 Off-line data organized for training and testing

Road Terrain Type	Training (m)		Testing (m)	
	Speed (km/h)	Distance (m)	Speed (km/h)	Distance (m)
Asphalt	20 ~ 40	1900	0 ~ 70	3948
Concrete	20 ~ 30	284	20 ~ 40	952
Grass	10	304	10 ~ 20	876
Gravel	20 ~ 30	1280	10 ~ 30	2712
Total		3768		8488

The Table 2 shows the classification results at different speeds. The first row shows the classification accuracies of Asphalt and Gravel tested at 40km/h (A40) and 10km/h (G10) while trained both at 20km/h (A20&G20) speed. Overall, the table shows very high accuracies leading to the conclusion that the LMS data is speed independent.

Table 2 Classification at different speeds

Training Speed (km/h)	**Testing Speed (km/h)**	***Asphalt Accuracy***	***Gravel Accuracy***
A20&G20	A40&G10	100.0%	99.2%
A20&G20	A30&G30	100.0%	100.0%
A20&G20	A30&G10	100.0%	99.2%
A30&G30	A20&G10	100.0%	100.0%
A30&G30	A40&G20	100.0%	100.0%

Classification Results based on Range Data

The training and testing data was all hand-labelled a priori. SVM classifier performed well on three road terrain types but not on the Asphalt road. As can be seen in Table 3, training with Asphalt and testing with all other road types has the worst accuracies. The Asphalt road has been heavily misclassified as Concrete road. This is mainly due

to the significant ambiguities between Asphalt features and Concrete features. In fact, those spatial frequency features just demonstrate that the surface structure of Asphalt road and Concrete road are very similar.

Table 3 Range data only

Training \ Testing	Asphalt	Concrete	Grass	Gravel
Asphalt	26.2%	39.3%	11.5%	23.0%
Concrete	0%	86.1%	13.9%	0%
Grass	0%	20.6%	76.7%	2.7%
Gravel	0%	2.3%	7.4%	90.3%
Average: 69.8%				

As for other three road terrain types, prediction accuracies of Concrete road, Grass road and Gravel road are 86.1%, 76.7% and 90.3% respectively. The structural differences obvious in gravel roads could be the reason for higher Gravel road classification accuracy. However, it could be noted that the overall average accuracy of road terrain type classification using LMS range data is just 69.8%.

The accelerometer data based classification reported in [Wang, 2012] has the problem of speed dependency. It required sufficiently large training data covering all speeds for better classification results. But if using LMS data, take this case for instance, it is not necessary to use all speed data in training phase but still provides a reasonable classification results.

Remission data

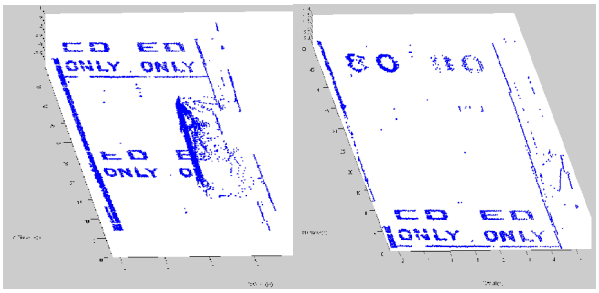

Fig. 7 Remission data

The reflection of a laser light is affected by object's surface properties and hence it is significantly affected by roadway scenes [Xiang, 2012]. The thresholded remission values of a certain data segment is shown in Fig. 7, where the blue points refer to reflective lane markings. In this particular scenario, the remission values can confuse the road type classifier. However in general, it performs well. That is because it can capture visual texture without being affected by environment lighting as does in camera images.

Classification based on Range and Remission data

The remission features were integrated to range features simply by combing Feature matrix (3) and feature matrix (4) to form a new feature matrix. All indices of samples were appropriately matched so that each range data sample corresponds to its remission data sample.

Table 4 Fusion of Range and Remission data

Training \ Testing	Asphalt	Concrete	Grass	Gravel
Asphalt	99.9%	0%	0%	0.1%
Concrete	0%	91.6%	8.4%	0%
Grass	0%	6.4%	93.6%	0%
Gravel	1.0%	0%	0.5%	98.5%
Average: 95.9%				

The same classifier with same parameters as in the previous section was used here. As expected, the classification accuracies of each class has increased. As can be seen in Table 4, accuracy of the Asphalt road classification has dramatically increased from 26.2% to 99.9%. It can be explained that the remission features helps to provide a clearer difference between all of the classes than that of range value only. The average classification accuracy was also improved to 95.9% with both range and remission features.

4 Conclusion

In this paper, we have presented a method to classify road terrain types based on LMS data. Range data was used to estimate road surface features and the remission data was used to extract another set of features. Fusion of both types of features lead to higher classification accuracies. It was also shown that the accuracies were speed independent within the given operating ranges of speeds.

We are currently working on online implementation and prediction of future road terrain types based on multi-sensor fusion algorithms.

Acknowledgment

This work is supported by the Centre for Autonomous Systems (CAS) and the Centre for Intelligent Mechatronic Systems (CIMS) of the University of Technology Sydney.

References

[Bouckaert, 2010] Remco R. Bouckaert, Eibe Frank, Mark A. Hall, Geoffrey Holmes, Bernhard Pfahringer, Peter Reutemann, and Ian H. Witten WEKA-Experiences with a Java Open-Source Project, *Journal of Machine Learning Research*, 11(2010)2533-2541, October 2010.

[Brooks, 2005] Christopher A. Brooks, Karl Iagnemma, Vibration-Based Terrain Classification for Planetary Exploration Rovers, *IEEE Transactions on Robotics*, 21(10) 1185-1191, December 2005.

[Dahlkamp, 2006] Hendrik Dahlkamp, Adrian Kaehler, David Stavens, Sebastian Thrun, Gary Bradski,

Self-Supervised Monocular Road Detection in Desert Terrain, T*he Robotics Science and Systems Conference*, August 2006

[Helmick, 2009] Daniel Helmick, Anelia Angelova, and Larry Matthies, Terrain Adaptive Navigation for Planetary Rovers, *Journal of Field Robotics*, 26(4):391-410 April 2009.

[Hsiao, 2009] Jen-Pin Hsiao, Cheng-Chung Hsu, Tzu-Chiang Shih, Pau-Lo Hsu, Syh-Shiuh Yeh, and Bor-Chyun Wang, The Real-time Video Stabilization for the Rescue Robot, *ICROS-SICE Int. Conf.*,pages 4364-4369, August 2009.

[Iagnemma, 2004] Karl Iagnemma, Shinwoo Kang, Hassan Shibly, and Steven. Dubowsky, Online terrain parameter estimations for wheeled mobile robots with application to planetary rovers, *IEEE Trans. Robot.* 20(5): 921-927, October 2004.

[Komma, 2009] Philoppe Komma, Christian Weiss, and Andreas Zell, Adaptive Bayesian Filtering for Vibration-based Terrain Classification, *IEEE Int. Conf. On Robots and Automation*, pages 3307-3313, May 2009.

[Luo, 2012] X. Luo, X. Ren, Y. Li, J. Wang, Mobile Surveying System for Road Assets Monitoring and Management, *IEEE Conference on Industrial Electronics and Applications (ICIEA)*, Singapore, July 2012.

[Nohse, 1991] Y. Nohse, K. Hashiguchi, M. Ueno, T. Shikanai, H. Izumi. A Measurement of Basic Mechanical Quantities of Off-The-Road Traveling Performance, *Journal of Terramechanics*, 28(4): 359-370, April 1992.

[Saitoh, 2010] Teppei Saitoh, Yoji Kuroda, Online Road Surface Analysis using Laser Remission Value in Urban Environments, *IEEE/RSJ International Conference on Intelligent Robots and Systems*, Taipei, Taiwan, October 18th-22nd 2010.

[Shmulevich, 1996] I. Shmulevich, D. Ronai, D. Wolf. A New Field Single Wheel Tester, *Journal of Terramechanics*, 33(3): 133-141, March 1996.

[Stavens, 2006] David Stavens, Sebastian Thrun, A Self-Supervised Terrian Roughness Estimator for Off-Road Autonomous Driving, *Conference on Uncertainty inAI (UAI)*, Cambridge, MA, USA, July 2006.

[Wang, 2011] Shifeng Wang, Sarath Kodagoda, Zhan Wang, Gamini Dissanayake, Multiple Sensor Based Terrian Classification, *Australasian Conference on Robotics and Automation (ACRA)*, Melbourne, Australia, December 7th-9th 2011.

[Wang, 2012] Shifeng Wang, Sarath Kodagoda, Rami Khushaba, Towards Speed-Independent Road-Type Classification, *International Conference on Control, Automation, Robotics and Vision (ICARCV)*, Guangzhou, China, December 5rd-7th 2012.

[Ward, 2009] Chris C. Ward, Karl Iagnemma, Speed-independent vibration-based terrain classification for passenger vehicles, *Vehicle System Dynamics*, 47(9):1095-1113, September 2009.

[Watson, 1984] D. F. Watson, G. M. Philip, Triangle Based Interpolation, *Mathematical Geology*, 16(8): October 1984.

[Weiss, 2007] Christian Weiss, Nikolas Fechner, Matthias Stark, and Andreas Zell, Comparison of Different Approaches to Vibration-based Terrain Classification, *European Conf. on Mobile Robots (ECMR*), pages *1-6, Freiburg, Germany*, 2007

[Weiss, 2008] Christian Weiss, Hashem Tamimi, and Andreas Zell, A Combination of Vision and Vibration-based Terrain Classification, IEEE/RSJ Int. Conf. On Intelligent Robots and Systems (IROS), pages 22-26, Nice, France, September 2008. Acropolis Convention Centre.

[Welch, 1967] P.D. Welch, The Use of Fast Fourier transform for the Estimation of Power Spectra: a Method Based on Time Averaging over Short, Modified Periodograms, *IEEE Trans*. Audio Electroacoust. AU-15:70-73, 1967.

[Wurm, 2009] Kai M. Wurm, Rainer Kümmerle, Cyrill Stachniss, and Wolfram Burgard, Improving Robot Navigation in Structured Outdoor Environments by Identifying Vegetation from Laser Data, *IEEE/RSJ Int. Conf. On Intelligent Robots and Systems (IROS)*, pages 1217-1222 October 2009.